A Theoretical Ab Initio Approach to the S−S Bond Breaking Process in Hydrogen Disulfide and in Its Radical Anion

Rois Benassi and Ferdinando Taddei*

Chemistry Department, University, Via Campi 183, 41100 Modena, Italy

Received: January 28, 1998; In Final Form: April 20, 1998

The S−S bond cleavage of dihydrogen disulfide, HSSH, and of its radical anion was studied theoretically with molecular orbital (MO) ab initio calculations at different levels of theory. The bond dissociation energy obtained from the total molecular energies of the undissociated HSSH and of the HS radicals is close to the best experimental value only with the G2 Møller−Plesset second-order perturbation (MP2) and complete basis set (CBS) methods and underestimated with the multiconfigurational self-consistent field (MCSCF) procedure regardless of the basis set and active space employed. The energy profile of the radical anion as a function of the S−S bond distance displays a minimum at 2.8 Å, and the activation energy for the electron transfer was calculated from the crossing of the energy profiles of the neutral molecule and of the radical anion both in the vapor phase and in media of different polarity. Changes in the activation energy of the order of 1 kcal/mol were found when transitions between vibrational levels of the S−S bond in the neutral molecule and in the radical anion were taken into account. A method for estimating the energy at the crossing point is proposed, based on Morse-like potential functions constructed from the second derivative of the calculated energies of the equilibrium structure of the neutral molecule and of the radical anion.

Introduction

The disulfide linkage, present in numerous proteins, enzymes, and antibiotics, plays an important role in stabilizing the structure and in determining the biological activity of the molecules.[1] These properties are related to the relative ease with which the S−S bond is broken and formed, and seeking an understanding of the mechanisms involved in these processes represents an interesting and worthwhile pursuit for biochemists, biologists, and organic and inorganic chemists. It is very important to know the oxidation and bond cleavage patterns in air-borne sulfur-containing pollutants in order to design strategies for their control and elimination.[2]

The scission of the S−S bond in RS−SR molecules can occur fundamentally in three ways: (1) through thermal bond dissociation, taking place in combustion processes; (2) through photochemical dissociation caused by an appropriate exciting wavelength; and (3) through one-electron reduction. From the first two processes the RS$^{\bullet}$ radical is obtained. The thermochemistry of several disulfides and of the radicals formed in their thermal dissociation has been investigated experimentally by Benson,[3] who also compiled tables of additive contributions for building up unknown thermodynamic properties. The photochemical fragmentation behavior of dimethyl disulfide has been reported[4,5] and the measured bond dissociation energies are in agreement with previous literature values.

The one-electron reduction of disulfides with a hydrated electron leads to a disulfide radical anion in equilibrium with the dissociated species:[6,7]

$$e^{-}_{aq} + R{-}S{-}S{-}R \rightarrow R{-}S{-}S{-}R^{\bullet -} \quad (1)$$

$$R{-}S{-}S{-}R^{\bullet -} \rightleftarrows RS^{\bullet} + RS^{-} \quad (2)$$

Radical anions of sulfur containing compounds have been observed in the pulse radiolysis of cystine and cysteamine,[8] hydrogen sulfide, and mercaptans.[9,10] Thermal and photochemical studies indicate that the sulfidryl radical and the anion form the complex $H_2S_2^{\bullet -}$, which has an association constant[11] of 2.5×10^4 M^{-1}. Electron paramagnetic resonance (EPR) studies emphasize the formation of this species in glassy matrixes[12,13] and on magnesium oxide.[14]

Theoretical studies provide useful information on the electronic mechanisms involved in the S−S bond cleavage, and a number of theoretical approaches, at different levels of theory, which predict the homolytic bond dissociation energies in disulfides have been reported.[14−16] Although theoretical approaches to the one-electron reduction and bond breaking of the carbon−halogen bond are available for methyl halides,[17−20] benzyl chloride,[21] and α,α,α-trichlorotoluene,[22] there appear to be few similar studies on compounds containing the S−S bond. For the halogenated derivatives the radical anion displays a purely dissociative character[17,18,21,22] and the reductive C−H$_{alg}$ bond cleavage is a concerted dissociative process. The activation energy for the electron transfer can be estimated from the forbidden crossing of the energy profiles of the neutral molecule and of the radical anion calculated as a function of the reaction coordinate. The value of the activation energy depends on the level of theory employed, and Møller−Plesset perturbation at least at second-order level (MP2)[23] is required[21,22] to obtain meaningful results. To locate the forbidden crossing, a number of calculations should be performed at different values of the reaction coordinate to construct the energy profiles of the neutral molecule and of the radical anion, and this is a very time-consuming process[21,22] even with molecules of medium molecular size (8−10 heavy atoms).

This paper aims to analyze the S−S bond cleavage process in thermal and one-electron reductive conditions at a theoretical level. Molecular orbital (MO) ab initio approaches at different levels of theory were chosen to test the effect of basis set, electron correlation by means of the Møller−Plesset perturbation

S1089-5639(98)00927-X CCC: $15.00
Published on Web 07/07/1998

TABLE 1: Total Molecular Energy (au) and Geometric Constants (Å, deg) for the Equilibrium Structure of Hydrogen Disulfide, Its Radical Anion, and Molecular Fragments Calculated at Different Theoretical Levels

H−S−S−H					
level of theory	*E*	S−S	S−H	S−S−H	H−S−S−H
MP2/3-21G*//MP2/3-21G*	−792.725631	2.058	1.341	99.06	90.19
MP2/3-21+G*//MP2/3-21+G*	−792.734814	2.068	1.341	98.27	90.47
MP2/6-31G*//MP2/3-21G*	−796.411274				
MP2/6-31G*//MP2/6-31G*	−796.411343	2.070	1.344	99.04	90.42
MP2/6-31+G*//MP2/6-31+G*	−796.414566	2.073	1.344	98.92	90.37
3-21G* MCSCF(2,2)	−792.497962	2.109	1.327	98.13	90.24
3-21G* MCSCF(14,10)	−792.540599	2.107	1.357	98.44	89.77
6-31G* MCSCF(14,10)	−796.232062	2.111	1.357	98.69	89.75
G2(MP2) energy	−796.677897	2.069	1.344	99.05	90.37
enthalpy	−796.641795				
CBS-4 energy	−796.692292	2.057	1.327	99.00	89.81
enthalpy	−796.669468				
CBS-q energy	−796.716762	2.057	1.327	99.00	89.81
enthalpy	−796.693938				
CBS-Q energy	−796.698421	2.071	1.344	99.03	90.39
enthalpy	−796.675486				
Experimental[a]		2.055	1.327	91.3	90.6
H−S−S−H$^{\bullet-}$					
level of theory	*E*	S−S	S−H	S−S−H	H−S−S−H
PMP2/3-21G*//MP2/3-21G*	−792.723832	2.824	1.340	84.86	102.54
PMP2/3-21+G*//MP2/3-21+G*	−792.753901	2.804	1.342	87.27	99.16
PMP2/6-31G*//MP2/3-21G*	−796.415073				
PMP2/6-31G*//MP2/6-31G*	−796.415091	2.830	1.344	85.80	100.63
PMP2/6-31+G*//MP2/6-31+G*	−796.430972	2.810	1.345	87.68	98.23
3-21G* MCSCF (3,2)	−792.481199	2.840	1.331	87.15	103.59
3-21G* MCSCF (15,10)	−792.519840	2.848	1.362	85.50	100.21
6-31G* MCSCF (15,10)	−796.213249	2.850	1.363	86.17	101.32
G2(MP2) energy	−796.696609	2.828	1.344	85.87	100.40
enthalpy	−796.676768				
CBS-4 energy	−796.713798	2.853	1.331	86.94	99.55
enthalpy	−796.693603				
CBS-q energy	−796.769486	2.853	1.331	86.94	99.55
enthalpy	−796.717369				
CBS-Q energy	−796.724172	2.829	1.334	85.84	100.53
enthalpy	−796.703960				

	E	
	HS$^{\bullet}$	HS^{-}
MP2/3-21G*//MP2/3-21G*	−396.319731[b]	−396.358331
MP2/3-21+G*//MP2/3-21+G*	−396.324823[b]	−396.390701
MP2/6-31G*//MP2/3-21G*	−398.163295[b]	−398.210441
MP2/6-31G*//MP2/6-31G*	−398.163299[b]	−398.210451
MP2/6-31+G*//MP2/6-31+G*	−398.164953[b]	−398.229605
G2(MP2) energy	−398.285357	−398.369960
enthalpy	−398.276155	−398.361051
CBS-4 energy	−398.293604	−398.377217
enthalpy	−398.284291	−398.368178
CBS-q energy	−398.307042	−398.390025
enthalpy	−398.297729	−398.380986
CBS-Q energy	−398.295855	−398.382779
enthalpy	−398.286485	−398.373704

[a] Ref 31. [b] PMP2 results.

theory,[23] and the inclusion of diffuse functions. The small HSSH molecule was chosen to test the effect of large basis sets and of the G2(MP2)[24] and complete basis set (CBS)[25] procedures with a view to applying the conclusions to larger molecular systems.

Computational Details

All ab initio calculations were performed with the Gaussian 92[26] and Gaussian 94[27] series of programs, run on an IBM AIX/6000 workstation. At the first level of approach, the electronic properties were obtained with different basis sets, 3-21G* and 6-31G*, diffuse augmented 3-21+G* and 6-31+G*, and correlation effects were calculated with the frozen core (fc) MP2 treatment. Stationary points were located through full geometry relaxation, and harmonic frequency calculations were also carried out. UHF wave functions were employed for the open shell systems and the spin-projection operator[28] was applied to remove contamination for higher spin states (results are reported as PMP2 values). The values of $<s^2>$ from the different approaches were in the interval 0.7668−0.7977, which reduce to 0.7502 after spin projection.

The bond-breaking process was examined with a multiconfigurational approach as well. The ab initio complete active space multiconfigurational self-consistent field (CAS MCSCF)

method with gradient optimization was employed with the 3-21G* and 6-31G* basis sets and two different active spaces (CAS). One active space includes only the σ and σ^* orbitals associated with the S−S bond, CAS(2,2) and CAS(2,3) in the neutral molecule and in the radical anion, respectively; in the other, 10 MOs were dealt with to allocate 14 or 15 (anion) electrons, CAS(14,10) and CAS(15,10) in the neutral molecule and in the radical anion, respectively. (The correction to the MCSCF energy due to dynamic correlation was evaluated by the MP2 treatment.)

Thermodynamic data can be obtained, within chemical accuracy (ca. 2 kcal/mol), from vibrational analysis employing general procedures.[23b] The G2(MP2)[24] approach has been shown to provide bond dissociation energies close to the best experimental or empirical values in disulfides[15] and in peroxides.[29] The CBS extrapolation[25] method was found[29] to perform remarkably well in reproducing bond dissociation energies of peroxides and was less time-consuming than the G2(MP2) method. The G2(MP2), CBS-4, CBS-q, and CBS-Q procedures were employed to compare the results from these methodologies for the disulfide linkage.

Force constants were calculated numerically in the energy minimum, at the same level of theory employed to derive the energy value.

Solvent effects were estimated through the self-consistent reaction field (SCFR) facility employing the isodensity polarized continuum model (IPCM) and vibrational frequency calculations were performed with the Onsager reaction field model, implemented on the Gaussian 94 package.[27]

Thermodynamic data refer to 298.15 K.

Results and Discussion

The fully relaxed geometry and the calculated total molecular energy for the ground state of the neutral HSSH molecule and its radical anion and also of the radicals and ions formed on breaking the bonds present in these molecules, obtained at the different levels of theory employed, are reported in Table 1. The most stable conformation is of the *skew* type (C_2 symmetry) for the neutral molecule and for the corresponding radical anion in all of the approaches employed. This orientation around the S−S bond seems to be a rather general feature of disulfides[15] with different substituents on the S atoms and of cyclic structures[30] with conformational freedom. The optimized geometric parameters of the ground state show a satisfactory agreement with experimental geometry.[31] The MCSCF results, when compared with those obtained from the other approaches, show greater S−S bond lengths, a trend observed previously for dimethyl disulfide.[32] A similar effect was found for the S−H bond, the length of which, for the minimal active space with the 3-21G* basis set, comes very close to the experimental value (1.327 Å). Bond and torsional angles obtained from the MCSCF approach differ to within 1° from the values calculated with the other approaches. Similar trends are found for the geometric parameters of the radical anion as well, with smaller differences between the values obtained by the different methods.

The homolytic bond dissociation energies (energy DE, enthalpy ΔH, and free energy ΔG) are obtained from the total energies of the undissociated molecule together with that of the molecular fragments formed after bond cleavage. In the multiconfigurational approach (MCSCF) the dissociation energy profile was constructed as a function of the S−S bond elongation (Figures 1 and 2) and the DE value refers to the difference between the energy of the equilibrium minimum and that corresponding to the fragments held at infinite S−S distance (assumed to be 10 Å). The calculated values are reported in Table 2.

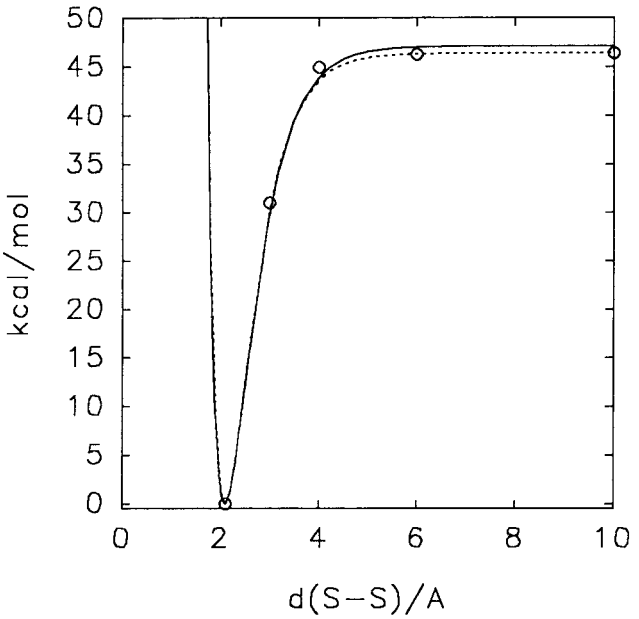

Figure 1. Diagrams of Morse-like potentials obtained for the HSSH molecule: full line refers to the fitting of MCSCF energies (3-21G* basis set, CAS(14,10)), and dashed line refers to the curve obtained with eq 3 and the *a* and *D* constants of Table 4 (see text).

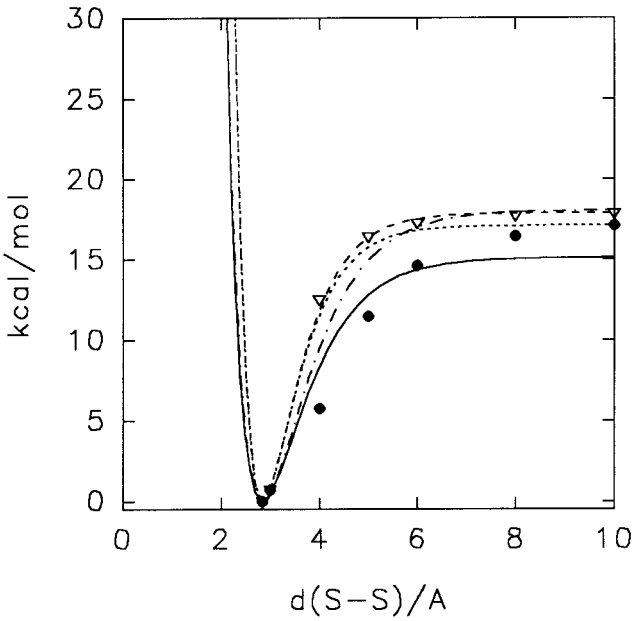

Figure 2. Diagrams of Morse-like potentials for the $HSSH^{\bullet -}$ molecule from different approaches: energy values (●) obtained without geometric constraints are interpolated with the (—) line, and the energy values (▽) obtained with geometrical constraints are interpolated with the (− · −) line; the energy profile (− −) was obtained from *k* and *D* derived from energy values with geometrical constraints, and the energy profile (···) from *k* and *D* values from energy values obtained without geometrical constraints.

The different levels of theory give entropy contributions that differ less than 1 kcal/mol and the discussion of the S−S bond cleavage can be restricted to the DE values.

The S−S bond dissociation energy for HSSH reported by Benson[3] amounts to 66 ± 2 kcal/mol. The MP2/3-21G* level underestimates the DE values with respect to this experimental determination. Basis set implementation at 6-31G* level both

TABLE 2: Bond Dissociation Energies DE, Enthalpies ΔH, Free Energies ΔG, in kcal/mol, of the S−S Bond in the HSSH Molecule and in Its Radical Anion at Different Levels of Theory

	H−S−S−H			H−S−S−H$^{\bullet-}$		
level of theory	DE	ΔH	ΔG	DE	ΔH	ΔG
MP2/3-21G*//MP2/3-21G*	54.07	51.40	41.92	28.72	27.57	20.67
MP2/3-21+G*//MP2/3-21+G*	53.44			24.08		
MP2/6-31G*//MP2/3-21G*	53.14			25.94		
MP2/6-31G*//MP2/6-31G*	53.18	50.54	41.48	25.94	24.83	17.95
MP2/6-31+G*//MP2/6-31+G*	53.12			22.85		
3-21G* MCSCF	43.65[a]			15.75[b]		
3-21G* MCSCF	46.39[c]			17.12[d]		
6-31G* MCSCF	45.64[c]			13.47[d]		
G2(MP2)	67.26	64.72	55.34	25.91	24.83	18.11
CBS-4	62.71	63.31	53.90	25.22	25.81	18.99
CBS-q	64.43	61.80	52.39	25.41	24.26	17.43
CBS-Q	66.96	64.33	54.92	28.57	27.47	20.70
Experimental[e]		66 ± 2				

[a] CAS(2,2). [b] CAS(3,2). [c] (CAS(14,10). [d] CAS(15,10). [e] Ref 2.

with MP2/3-21G* relaxed molecular geometry or at MP2/6-31G*//MP2/6-31G* level does not provide appreciable changes in the calculated DEs (which range between 53.14 and 53.18 kcal/mol). Inclusion of diffuse functions does not significantly improve the results. The DE values calculated at this level of theory[15] for a series of symmetrical and unsymmetrical substituted disulfides, though underestimated, showed a remarkable proportionality with experimental or empirical values.

DE values obtained with the MCSCF approach are underestimated as well, regardless of the basis set and active space employed. The introduction of dynamic correlation corrections at the MP2 level and the 3-21G* basis set for the neutral HSSH molecule gives DE values of 56.14 kcal/mol, CAS(2,2), and 54.03 kcal/mol, CAS(14,10).

Calculated DE values close to the experimental ones are obtained with the G2(MP2) and CBS procedures. These procedures nevertheless require long computational times, and their application to large molecules is rather problematic, especially when a number of energy values are required in order to scan the potential energy surface.

For the radical anion, all of the calculation procedures employed indicate that a minimum equilibrium structure is present with a rather long S−S bond length (2.824−2.850 Å). It has been suggested,[6−14] on the basis of a number of experimental determinations, that hydrogen disulfide and disulfides of higher molecular complexity form a radical anion complex, with a similar S−S bond length.

The relative stability of the radical anion and of the neutral molecule depends on the calculation approach employed (Table 3). In the MP2/3-21G*//MP2/3-21G* scheme the neutral molecule is more stable than the radical anion, but with the more extended 6-31G* basis set this order of stability is inverted. The neutral molecule is more stable (10 kcal/mol) even at the MCSCF level. The stability of the radical anion becomes markedly higher than that of the neutral molecule, more than 13 kcal/mol, with the G2(MP2) and CBS codes. Inclusion of diffuse functions, 3-21+G* and 6-31+G* basis sets, has a marked effect on increasing the stability of the radical anion yet the effect is small on the neutral molecule. The ΔE_0 values become closer to those obtained with the G2(MP2) and CBS protocols. The same conclusions stem from the enthalpy ΔH_0 and free energy ΔG_0 of the process.

The energy required for the adiabatic one-electron transfer of the HSSH molecule (vertical electron affinity) is reported in Table 3 as well. The inclusion of diffuse functions has the effect of lowering the negative of the vertical electron affinity (VEA).

TABLE 3: Relative Stability,[a] in kcal/mol, of the HSSH Molecule and of Its Radical Anion[b] and Vertical Electron Affinity (VEA) (kcal/mol) at Different Levels of Theory

level of theory	ΔE_0	ΔH_0	ΔG_0	VEA
MP2/3-21G*//MP2/3-21G*	1.13	−0.52	−2.69	−49.43
MP2/3-21+G*//MP2/3-21+G*	−11.98			−19.86
MP2/6-31G*//MP2/3-21G*	−2.38			
MP2/6-31G*//MP2/6-31G*	−2.35	−4.05	−5.82	−39.79
MP2/6-31+G*//MP2/6-31+G*	−10.29			−19.55
3-21G* MCSCF	10.52[c]			−54.89
3-21G* MCSCF	13.03[d]			−57.19
6-31G* MCSCF	11.81[d]			−53.50
G2(MP2)	−11.74	−13.38	−15.64	
CBS-4	−13.49	−15.14	−17.33	
CBS-q	−13.05	−14.70	−16.89	
CBS-Q	−16.16	−17.87	−20.11	

[a] Total molecular energy ΔE_0 (PMP2 for the radical anion), enthalpy ΔH_0, and free energy ΔG_0. [b] Negative values indicate a greater stability of the radical anion. [c] CAS(2,2) for the neutral molecule and CAS(3,2) for the radical anion. [d] CAS(14,10) for the neutral molecule and CAS(15,10) for the radical anion.

This result should depend on the fact that diffuse augmented functions significantly improve the description of antibonding orbitals.

In Table 2 the dissociation energies of the radical anion complex, according to eq 2, are reported. HF/MP2, G2(MP2), and CBS provide close values (24−29 kcal/mol), but those from MCSCF are approximately 10 kcal/mol smaller. Diffuse functions have a small effect on the dissociation energy of the radical anion and this should depend on the fact that their inclusion in the 3-21G* and 6-31G* basis sets lowers the molecular energy of the radical anion and of the HS^- fragment of a similar quantity.

The energy profiles of the S−S bond dissociation of the neutral molecule and of the corresponding radical anion complex enable the one-electron transfer and bond-breaking mechanisms to be more closely examined and the activation energy for the electron transfer to be estimated. The evaluation of the energy profile as a function of S−S bond stretching with the HF/MP2 method is complicated by self-size consistence.[28a,28b,33] The most coherent way of constructing the dissociation energy profile is represented by the MCSCF approach, and this was adopted employing a 3-21G* basis set with a CAS(2,2) and CAS(14,10) for the neutral molecule and a CAS(3,2) and CAS-(15,10) for the radical anion. In Figures 1 and 2 the curves obtained for the two systems with the more extended CAS are reported (the minimal CAS gives similar profiles).

TABLE 4: Parameters Entering into the Morse Equation (eq 3) for the HSSH Molecule[a]

	interpolated values[b]			calculated from vibrational frequencies[b]		
level of theory	*a*	*D*	*k*	*a*	*D*	*k*
MP2/3-21G*//MP2/3-21G*				1.026	0.086169	0.1816
MP2/3-21+G*//MP2/3-21+G*				1.017	0.085168	0.1760
MP2/6-31G*//MP2/6-31G*				1.048	0.084744	0.1862
MP2/6-31+G*//MP2/6-31+G*				1.046	0.084659	0.1851
3-21G* MCSCF (2,2)	1.025	0.069857	0.1467	1.015	0.069560	0.1434
3-21G* MCSCF (14,10)	0.938	0.075114	0.1321	0.975	0.073935	0.1407
6−31G* MCSCF (14,10)				1.017	0.072733	0.1505
G2(MP2)				0.953	0.102193	0.1855
CBS-4				0.986	0.099412	0.1194
CBS-q				0.998	0.097533	0.1942
CBS-Q				0.956	0.101571	0.1859

[a] *a* in Bohrs$^{1/2}$; *D* in au; *k* in Hartree−Bohrs. [b] From the second derivative of the molecular energy (see text).

TABLE 5: Parameters Entering into the Morse Equation (eq 3) the HSSH$^{\bullet-}$ Molecule[a]

	interpolated values[b]			calculated from vibrational frequencies[b]		
level of theory	*a*	*D*	*k*	*a*	*D*	*k*
PMP2/3-21G*//PMP2/3-21G*				0.598	0.045770	0.0327
PMP2/3-21+G*//PMP2/3-21+G*				0.636	0.038377	0.0310
PMP2/6-31G*//PMP2/6-31G*				0.590	0.041336	0.0288
PMP2/6-31+G*//PMP2/6-31+G*				0.618	0.036414	0.0278
3-21G* MCSCF (3,2)[c]	0.642	0.021411	0.0177	0.846	0.025107	0.0360
3-21G* MCSCF (3,2)[d]	0.606	0.026908	0.0198	0.825	0.026440	0.0360
3-21G* MCSCF (15,10)[c]	0.622	0.024110	0.0187	0.791	0.027287	0.0341
3-21G* MCSCF (15,10)[d]	0.595	0.028785	0.0203	0.774	0.028501	0.0341
6-31G* MCSCF (15,10)				0.841	0.021469	0.0304
G2(MP2)				0.607	0.038618	0.0285
CBS-4				0.646	0.040191	0.0336
CBS-q				0.667	0.037709	0.0336
CBS-Q				0.580	0.042826	0.0288

[a] *a* in Bohrs$^{1/2}$; *D* in au; *k* in Hartree−Bohrs. [b] See text. [c] Energy values obtained without geometry restrictions were employed in the interpolation (see text). [d] Energy values with the geometry restrictions were employed in the interpolation (see text).

The pattern of calculated energies for the HSSH and HSSH$^{\bullet-}$ molecules is typical of a Morse-like potential function, eq 3:

$$u(r) = D[1 - e^{-a(r-r_e)}]^2 \quad (3)$$

where r_e is the equilibrium length of the S−S bond. The *a* and *D* constants reported in Table 4 were obtained by fitting the calculated energy values to eq 3, and the corresponding plot is reported in Figure 1 as a continuous line. The values of *D*, compared with the DE values reported in Table 2, are slightly greater.

In principle, the *a* values can also be obtained by an approximate approach based on the vibrational analysis of a biatomic oscillating system,[34] where, in large molecules, the two masses are simply assumed to be those of the atoms at the ends of the bond to be broken.

The constant *a* has the form (4):

$$a = (k/2D)^{1/2} \quad (4)$$

where *k*, the force constant, is the second derivative of the potential function at equilibrium distance $r = r_e$.

The second derivative with respect to the S−S bond length coordinate was calculated by numerical differentiation, and the values of *k* are reported in Table 4. These values can be compared with those obtained directly from the interpolated Morse-like function and reported in Table 4 as well. The potential energy profile obtained by employing the values of *k* from eq 5 is plotted in Figure 1 as a dashed line.

$$k = (\delta^2 u/\delta r^2)_{r=r_e} \quad (5)$$

The energy profile for the radical anion (Figure 2) is similar in its behavior to that of the neutral molecule, albeit different for a number of features. The energy values calculated at fixed values of the S−S bond distance and by relaxing all of the remaining coordinates are not satisfactorily interpolated by a Morse equation of type 3 and do not fit properly those coordinates given by the *a* and *D* values reported in Table 5 for this molecule. The reason for this unexpected behavior became clear when the geometric features at the different S−S bond distances of the radical anion were examined. For S−S distances smaller than 3 Å, the radical anion has a structure very similar to that of the neutral molecule, a first minimum occurring at 2.8 Å (minimum A). Further stretching of the bond (up to 4 Å) causes one S−S−H bond angle to bend sharply, while a hydrogen atom interposes itself between the two sulfur atoms, corresponding to a second minimum (minimum B, drawn in Figure 3). This orientation does not change when the S−S bond distance is further increased. The failure of the proper interpolation of the energy values with the Morse equation is likely to originate from this geometric distortion.

An almost planar equilibrium structure, with one hydrogen atom interposed between the oxygen atoms, has been observed[35] in an MCSCF study of the O−O bond cleavage of hydrogen peroxide radical anion. Whereas for the radical anion of dihydrogen peroxide, this is the global minimum[36] for the radical anion of the corresponding disulfide the relative stability of the two minima are reversed. At the MCSCF level with a CAS-(15,10) the minimum B is 4.69 kcal/mol less stable than A with the 3-21G* basis set and 2.73 kcal/mol less stable with the 6-31G* basis set. The energy minimum of type B is not observed when the other theoretical approaches are employed.

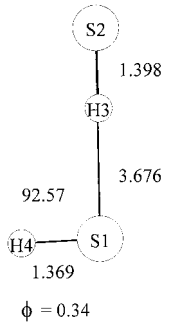

Figure 3. Calculated molecular geometry of the minimum of the $HSSH^{\bullet-}$ molecule showing one hydrogen atom interposed between the sulfur atoms (minimum B). Bond lengths and bond angle at 6-31G* MCSCF (CAS 15,10) level, $E = -796.208904$ au. ϕ is the SHSH dihedral angle.

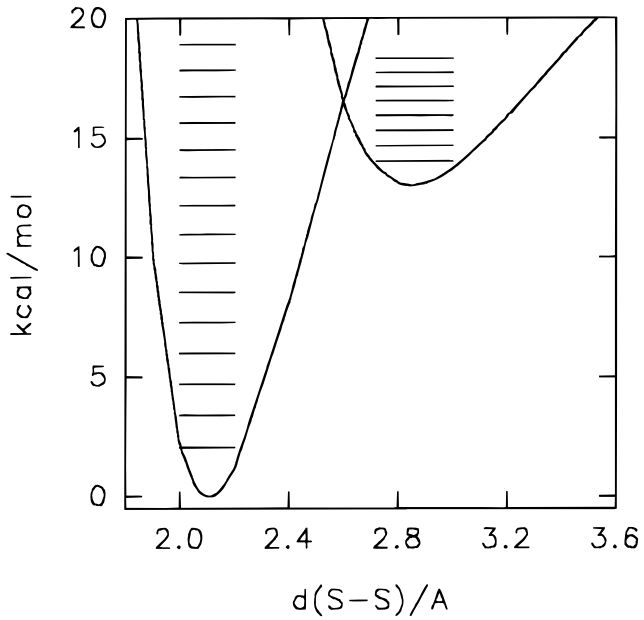

Figure 4. Graphical representation of the intersection between the energy profile of the HSSH molecule and that of the radical anion with the vibrational levels relative to the S−S bond (MCSCF calculations with the 3-21G* basis set).

To examine the energy profile of S−S bond cleavage independently of the recombination process of the SH fragments with hydrogen shift, energy values were calculated as a function of the S−S distance with geometric constraints. Applying the interpolating Morse eq 3 to these values, the fit is as satisfactory as in the neutral molecule. The DE value calculated from this approach is 0.8 kcal/mol greater than that obtained from the energies corresponding to complete molecular relaxation.

Accordingly, constants *a* and *D* from the energies calculated at different levels of theory were employed to study the process described by eq 1. The activation energy for the one-electron transfer can be estimated from the crossing of the energy curves of the neutral molecule and of the radical anion, constructed through eq 3 and the constants reported in Tables 4 and 5. A free electron not contributing to the total energy of the neutral molecule is assumed to be present. A graphical example is depicted in Figure 4, and the numerical values of the energy (E_C) and S−S bond distance (d_C) in the crossing point are reported in Table 6. The E_C values are rather sensitive to the theoretical method employed and range over a wide energy interval (4−16 kcal/mol) but the d_C values obtained with the HF/MP2 and CBS protocols span a relatively narrow interval (2.30−2.24 Å). The MCSCF results differ sharply from the

TABLE 6: Activation Energy E_C [a] and Corrected for Vibrational Levels E_{FC}, S−S bond d_e Distance at the Crossing Point between the Energy Profiles of HSSH and of Its Radical Anion

level of theory	E_C [b]	d_C [c]	E_{FC} [b]	$\Delta\Delta v$ [h]
MP2/3-21G*//MP2/3-21G*	12.39	2.394	12.49	0.13
MP2/3-21+G*//MP2/3-21+G*	6.30	2.282	6.71	0.09
MP2/6-31G*//MP2/6-31G*	10.06	2.358	11.23	0.12
MP2/6-31+G*//MP2/6-31+G*	6.17	2.283	6.88	0.04
3-21G* MCSCF[d,e]	15.07	2.571	15.67	0.10
3-21G* MCSCF[f,e]	15.05	2.570	15.67	
3-21G* MCSCF[d,g]	16.50	2.599	16.75	0.17
3-21G* MCSCF[f,g]	16.48	2.599	16.75	
6-31G* MCSCF[d,g]	15.87	2.575	16.08	0.098
G2(MP2)	6.13	2.275	6.93	0.064
CBS-4	8.33	2.300	8.59	0.22
CBS-q	8.61	2.307	10.08	0.23
CBS-Q	4.38	2.239	5.43	0.17

[a] Referring to the minimum of the neutral molecule. [b] In kcal/mol. [c] In Å. [d] Energy values obtained without geometry restrictions were employed in the interpolation (see text). [e] CAS(2,2) for the neutral molecule and CAS(3,2) for the radical anion. [f] Energy values with the geometry restrictions were employed in the interpolation (see text). [g] CAS(14,10) for the neutral molecule and CAS(15,10) for the radical anion. [h] $\Delta\Delta v$ is the energy difference between the nearest vibrational levels in the region of the crossing point.

TABLE 7: Fundamental Frequency v_e (cm^{-1}) and First Vibrational Transition $\Delta v_{0\to1}$ (cm^{-1}) in HSSH and in Its Radical Anion

	HSSH		$HSSH^{\bullet-}$	
level of theory	v_e	$\Delta v_{0\to1}$	v_e	$\Delta v_{0\to1}$
MP2/3-21G*//MP2/3-21G*	547.87	539.94	232.63	229.94
MP2/3-21+G*//MP2/3-21+G*	539.20	531.43	226.40	223.36
MP2/6-31G*//MP2/6-31G*	554.71	546.43	218.07	215.45
MP2/6-31+G*//MP2/6-31+G*	553.17	544.94	214.52	211.64
3-21G* MCSCF[b]	486.83	479.07	243.87	238.47
3-21G* MCSCF[c]	482.19	475.03	237.59	232.88
6-31G* MCSCF[c]	498.71	490.92	224.09	218.76
G2(MP2)	553.77	546.93	218.98	216.15
CBS-4	566.65	559.33	235.53	232.38
CBS-q	566.65	559.14	235.53	232.18
CBS-Q	554.29	547.40	218.22_5	215.69
3-21G*	549.69[a]		230.90[a]	
MP2/3-21G*	529.30[a]		226.26[a]	
6-31G*	568.44[a]		212.81[a]	
MP2/6-31G*	539.09[a]		211.52[a]	

[a] Values obtained from a complete vibrational analysis. [b] CAS(2,2) for the neutral molecule and CAS(3,2) for the radical anion. [c] CAS(14,10) for the neutral molecule and CAS(15,10) for the radical anion.

results of the other approaches both for the E_C (15−16 kcal/mol) and d_C values (2.6 Å). The energy in the crossing point depends mainly on the relative stability of the radical anion and of the neutral molecule (Table 3): the activation energy (E_C) is smaller when the product, radical anion, is more stable than the reagent. The comparison of the HF/MP2 and CBS results clearly shows that they afford very similar equilibrium structures, but the calculated relative stability is rather different. The pathway of the process described by the different approaches is nevertheless qualitatively the same: an intermediate radical anion is formed through an activation step and the energy required by the radical anion to reach the crossing point is lower than that required for its dissociation.

To check the reliability of the energy values obtained analytically from the intersection of the two curves, the molecular energies of the neutral molecule and the radical anion in the crossing point were computed at MP2/3-21G*//MP2/3-21G* and MP2/6-31G*//MP2/6-31G* levels. Geometry relaxation was performed with the constraint of a constant S−S bond

TABLE 8: Calculated Solvent Effect (See Text) in Media of Different Permittivity ϵ on the Dissociation Energy DE, on the Relative Stability ΔE_0 of HSSH and of Its Radical Anion,[a,b] and on the Association Constant K [c]

MP2/3-21G*							
ϵ	DE(HSSH)	DE(HSSH$^{\bullet-}$)	ΔE_0 (HSSH−HSSH$^{\bullet-}$)	d_C	E_C	E_{FC}	K
							6.5×10^{13} [d]
4.83	53.52	18.05	44.87	2.153	1.53	2.32	9.2×10^5
9.08	53.41	16.70	50.51	2.139	1.15	2.32	9.4×10^4
20.7	53.33	15.83	54.11	2.132	0.98	2.32	2.1×10^4
37.5	53.31	15.53	55.37	2.130	0.93	2.32	1.3×10^4
78.0	53.21	15.30	56.18	2.129	0.90	2.32	8.8×10^3
MP2/6-31G*							
ϵ	DE(HSSH)	DE(HSSH$^{\bullet-}$)	ΔE_0 (HSSH−HSSH$^{\bullet-}$)	d_C	E_C	E_{FC}	K
							6.5×10^{11} [d]
4.83	52.65	15.86	47.71	2.123	0.54	2.35	2.5×10^4
9.08	52.56	14.38	52.24	2.112	0.34	2.35	2.0×10^3
20.7	52.60	13.53	56.76	2.107	0.27	2.35	4.8×10^2
37.5	52.47	13.24	57.99	2.105	0.25	2.35	3.0×10^2
78.0	52.39	13.05	58.85	2.104	0.23	2.35	2.1×10^2

[a] All energy values in kcal/mol. [b] For the definition of E_C, d_C, and E_{FC} quantities (see Table 6). [c] In M^{-1}. [d] Vapor phase.

length, assumed to be equal to the d_C values reported in Table 6. The differences between the directly calculated total energies and the interpolated E_C values amount to less than 1 kcal/mol. These results seem to support the correctness of the methodology employed to evaluate the energy profile of the bond dissociation process.

In deriving the energy of activation of the one-electron transfer from the crossing of the two energy profiles we should remember that Franck−Condon restrictions need to be satisfied.[36] An effective transition from a vibrational level of the neutral molecule to a corresponding level of the radical anion occurs only when the two levels have nearly equal energy, namely in the zone of maximum overlap of their vibrational wave functions. In the remaining zones the overlap and the perturbation are small. The zone of maximum overlap starts, in our case, from the crossing point of the energy profiles. An analysis of the vibrational levels involved in the S−S bond stretching can be carried out by employing the solutions of the radial equation, using the Morse potential.[34] The vibrational frequency of the molecule is given by:

$$\upsilon_e = (1/2\pi c)\sqrt{(k/\mu)} \qquad (6)$$

where k is the force constant and μ the reduced mass of the two S atoms. Disregarding the rotational terms, the vibrational energy levels can be expressed with eq 7:

$$\epsilon_V = hc[\upsilon_e(\upsilon + 1/2) - x_e\upsilon_e(\upsilon + 1/2)^2] \qquad (7)$$

where $x_e = hc\upsilon_e/4D$ is an anharmonicity term. The values of υ_e obtained with the k values of Tables 4 and 5 and the value of the first vibrational transition are reported in Table 7, and compare satisfactorily with the experimental S−S stretching of the HSSH molecule (509 cm^{-1}).[37] The stretching of the S−S bond obtained from the complete vibrational analysis carried out at the different levels of theory is fairly close to the frequency value determined with eq 7.

By employing the vibrational energy levels obtained from eq 7 and depicted in a graphical form in Figure 4, it was possible to determine a new E_C value (E_{FC} in Table 7) fulfilling the requirement of the interaction between vibrational levels of similar energy. The calculation of E_{FC} refers to the level of the neutral molecule closest to the crossing point and to that of the radical anion differing by 0.1−0.2 kcal/mol from that chosen for the neutral molecule. The E_{FC} values differ by ∼1 kcal/mol from those evaluated from the crossing of the energy profiles. The estimate of the activation energy for the one-electron transfer thus seems accurate enough, even without taking the vibrational correction into account. This holds for high values of the quantum number υ. The vibrational level involved in the radical anion lies below the dissociation limit and, once the electron transfer has occurred, the molecule relaxes to the fundamental vibrational state.

The results discussed above refer to the molecules in the vapor phase, but the majority of experimental results were obtained in the condensed phase. Calculations simulating the solvent effect were performed with the IPCM solvation model at MP2/3-21G*//MP2/3-21G* and MP2/6-31G*//MP2/6-31G* levels of theory. The free electron is replaced in this case by a solvated (hydrated in water) electron. The results obtained simulating solvents of increasing dielectric constants are reported in Table 8. The solvent effect is rather small for the neutral molecule and radicals and the calculated DE values differ by within 1 kcal/mol with respect to the vapor phase for the two basis sets employed. The calculated solvent effects are definitely marked for the radical anion. In a solvent of low polarity ($\epsilon = 4.83$) the DE value becomes about 10 kcal/mol lower than in the vapor phase, and this difference increases gradually as the polarity of the medium increases. This behavior is common to the two basis sets. The highest solvent effect is on the relative stability of the neutral molecule and of the radical anion (ΔE_0 in Table 8), the charged molecule being at least 50 kcal/mol more stable than the neutral one. The activation energy is strictly related to the ΔE_0 values and decreases in a similar fashion.

Assuming that force constants are not significantly affected by solvents, solvent dependent energy profiles were calculated by inserting the new DE values (Table 8) in eqs 3 and 4. A graphical example is reported in Figure 5. The d_C and E_C values at the crossing point are smaller than those obtained in the vapor phase (Table 8).

The reliability of the assumptions made in this treatment was tested through complete frequency analysis in all the molecular species involved, with inclusion of the solvent and with the 6-31G* basis set. The molecular geometry was completely relaxed simulating a solvent with a dielectric constant $\epsilon = 80$. The frequencies calculated in the presence of solvent differ by less than 1 cm^{-1} from those of the free molecule both for HSSH and HSSH$^{\bullet-}$. The frequency of the S−S stretching amounts to 568.75 cm^{-1} in the disulfide and 212.43 cm^{-1} in its radical

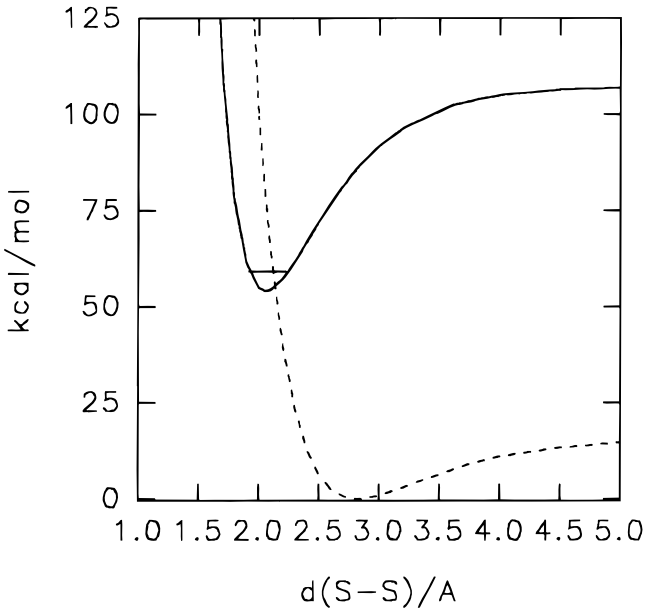

Figure 5. Graphical representation of the energy profiles of the HSSH molecule and of its radical anion in a solvent with $\epsilon = 20.7$ (dashed line). Energy values are at the MP2/6-31G* level.

anion. The vibrational level of the S−S bond in the ground state of the radical anion is now much lower than that of the neutral molecule (Figure 5). The results from the study of the solvent effect again support the presence of a transition state for the one-electron transfer. The energy of the crossing point (E_C) is higher than that corresponding to the dissociated species, and the radical anion should undergo direct ground-state fragmentation. Nevertheless, the presence of a flat minimum, even in solution, would agree with a recombination process due to reversal of reaction 2. The formation of $HSSH^{\bullet-}$ in aqueous solution has been demostrated by pulse radiolysis experiments.[11]

From the analysis of the vibrational levels it emerges that the crossing point for the neutral molecule lies below the first vibrational level for all of the solvents examined, and that the calculated E_{FC} assumes a value independent of the solvent.

In conclusion, the calculation of the activation energy for the electron transfer bond breaking process from the crossing of the energy profiles of the neutral molecule and of the radical anion, as determined from the energy of the equilibrium structure, seems to give reliable results. The procedure applies satisfactorily when the energy profile of the radical anion is described by a Morse-like energy profile, and saves computational time with respect to the construction of energy profiles from a number of calculations at different bond distances. Taking into account the transitions between vibrational levels of the S−S bond, corrections to the energy of activation are of the order of 1 kcal/mol for the molecules in the vapor phase. In solution, the anion becomes more stable than the neutral molecule and its energy of dissociation decreases with respect to the vapor phase.

The free energy ΔG for the dissociation of $H_2S_2^{\bullet-}$ allows us to estimate the association constant of this ion-radical complex. The values of K reported in Table 8 show that the high value calculated for the vapor phase decreases in solution and becomes of the order of magnitude of the experimental value.[11]

Acknowledgment. This work was financially supported by the Italian Ministero dell′ Università e della Ricerca Scientifica e Tecnologica (MURST).

References and Notes

(1) Huxtable, R. J. *Biochemistry of sulphur*; Plenum Press: New York, 1986.
(2) Cullis, C. F.; Mulcahy, M. F. R. *Comb. Flame* **1975**, *18*, 225.
(3) Benson, S. W. *Chem. Rev.* **1978**, *78*, 23.
(4) (a) Callear, A. B.; Dickon, D. R. *Trans. Faraday Soc.* **1970**, *66*, 1907. (b) Rao, P. M.; Copeck, J. A.; Knight, A. R. *Can. J. Chem.* **1967**, *45*, 1369. (c) Samayol, K.; Knight, A. R. *Can. J. Chem.* **1969**, *46*, 999. (d) Rao, P. M.; Knight, A. R. *Can. J. Chem.* **1969**, *46*, 2462.
(5) Nourbaksh, S.; Liao, C.-L.; Ng, C. Y. *J. Chem. Phys.* **1990**, *92*, 6587.
(6) Purdie, J. W.; Gillis, H. A.; Klassen, N. V. *Can. J. Chem.* **1973**, *51*, 3132.
(7) Hoffman, M. Z.; Hayon, E. *J. Am. Chem. Soc.* **1972**, *94*, 7957.
(8) Mezyk, S. P. *Chem. Phys. Lett.* **1995**, *235*, 89.
(9) Karmann, W.; Meissner, G.; Henglein, A. Z. *Naturforsch* **1967**, *B22*, 273.
(10) Karmann, W.; Granzow, A.; Meissner, G.; Henglien, A. *Int. J. Radiat. Phys. Chem.*, **1969**, *1*, 395.
(11) Mills, G.; Schmidt, K. H.; Matheson, M. S.; Meisel, D. *J. Phys. Chem.* **1987**, *91*, 1590.
(12) Lin, M. J.; Lunsford J. H. *J. Phys. Chem.* **1976**, *80*, 2015.
(13) Zhu, J.; Petit, K.; Colson, A. O.; DeBolt, S.; Sevilla, M. D. *J. Phys. Chem.* **1991**, *95*, 3676.
(14) Benassi, R.; Fiandri, G. L.; Taddei, F. *Tetrahedron* **1994**, *43*, 12469.
(15) Benassi, R.; Fiandri, G. L.; Taddei, F. *J. Mol. Struct. (THEOCHEM)* **1997**, *418*, 127.
(16) Fournier, R.; DePristo, A. E. *J. Chem. Phys.* **1995**, *96*, 1183.
(17) Benassi, R.; Bernardi, F.; Bottoni, A.; Robb, M. A.; Taddei, F. *Chem. Phys. Lett.* **1989**, *161*, 179.
(18) Bertran, J.; Gallardo, I.; Moreno, M.; Saveant, J. M. *J. Am. Chem. Soc.* **1992**, *114*, 9576.
(19) Tada, T.; Yoshimura, R. *J. Am. Chem. Soc.* **1992**, *114*, 1503.
(20) German, E. D.; Kuznestov, A. M.; Tikhomirov, V. A. *J. Phys. Chem.* **1995**, *99*, 9095.
(21) Benassi, R.; Bertrarini, C.; Taddei, F. *J. Phys. Chem.* **1995**, *99*, 9095.
(22) Benassi, R.; Bertarini, C.; Taddei, F. *J. Chem. Soc., Perkin Trans. 2* **1997**, 2263
(23) (a) Møller, C.; Plesset, M. S. *Phys. Rev.* **1934**, *46*, 618. (b) Hehre, W. J.; Radom, L.; Schleyer, P. v. R.; Pople, J. A. *Ab initio Molecular Orbital Theory*; John Wiley & Sons: New York, 1986.
(24) Curtiss, L. A.; Raghavachari, K.; Trucks, G. W.; Pople, J. A. *J. Chem. Phys.* **1991**, *94*, 7221.
(25) (a) Petersson, G. A.; Tensfeldt, T. G.; Montgomery, J. A. *J. Chem. Phys.* **1991**, *94*, 6091. (b) Montgomery, J. A.; Ochterski, J. W.; Petersson, G. A.; *J. Chem. Phys.* **1994**, *101*, 5900. (c) Ochterski, J. W.; Petersson, G. A.; Wiberg, K. B. *J. Am. Chem. Soc.* **1995**, *117*, 11299. (d) Ochterski, J. W.; Petersson, G. A.; Montgomery, J. A. *J. Chem. Phys.* **1996**, *104*, 2598.
(26) Frisch, M. J.; Trucks, G. W.; Head-Gordon, M.; Gill, P. M. W.; Wong, M. W.; Foresman, J. B.; Johnson, B. G.; Schlegel, H. B.; Robb, M. A.; Repogle, E. S.; Gomberts, R.; Andres, J. L.; Raghavachari, K.; Binkley, J. S.; Gonzales, C.; Martin, R. L.; Fox, D. J.; Defrees, D. J.; Baker, J.; Stewart, J. J. P.; Pople, J. A. Gaussian 92, Revision C; Gaussian Inc.: Pittsburgh, PA, 1992.
(27) Frisch, M. J.; Trucks, G. W.; Head-Gordon, M.; Gill, P. W.; Wong, M. W.; Foresman, J. B.; Johnson, B. G.; Schlegel, H. B.; Robb, M. A.; Repogle, E. S.; Gomberts, R.; Andres, J. L.; Raghavachari, K.; Binkley, J. S.; Gonzales, C. R.; Martin, L.; Fox, D. J.; Defrees, D. J.; Baker, J. T.; Keith, A.; Petersson, G. A.; Montgomery, J. A.; Al-Laham, M. A.; Zakrzewski, V. G.; Ortiz, J. V.; Cioslowski, J.; Stefanov, B. B.; Nanayakkara, A.; Challacombe, M.; Peng, C. Y.; Ayala, P. Y.; Chen, W.; Stewart, J. J. P.; Pople, J. A. Gaussian 94, Revision A.1; Gaussian Inc.: Pittsburgh, PA, 1995.
(28) (a) Schlegel, H. B. *J. Chem. Phys.* **1986**, *84*, 4530. (b) Schlegel, H. B. *J. Chem. Phys.* **1988**, *92*, 3075. (c) Sosa, C.; Schlegel, H. B. *Int. J. Quantum Chem.* **1986**, *29*, 1001. (d) Sosa, C.; Schlegel, H. B. *Int. J. Quantum Chem.* **1986**, *30*, 155.
(29) Bach, R. D.; Ayala, P. Y.; Schlegel, H. B. *J. Am. Chem. Soc.* **1996**, *118*, 12578.
(30) Po, H. N.; Freeman, F.; Lee, C.; Hehre, W. J. *J. Comput. Chem.* **1993**, *14*, 1376.
(31) Winnewisser, G.; Winnewisser, M.; Gordy, W. *J. Chem. Phys.* **1968**, *49*, 3465.
(32) Benassi, R.; Fiandri, G. L.; Taddei, F. *J. Mol. Struct. (THEOCHEM)*, **1993**, *279*, 239.
(33) Benassi, R.; Taddei, F. *Tetrahedron* **1994**, *50*, 4795.
(34) Daudel, R.; Leroy, G.; Peeters, D.; Sana, M. *Quantum Chemistry*; John Wiley and Sons: Chichester, 1983.
(35) Benassi, R.; Taddei, F. *Chem. Phys. Lett.* **1993**, *204*, 595.
(36) King, W. K. *Spectroscopy and Molecular Structure*; Holt, Rinehart and Winston, Inc.: New York, 1964.
(37) Shimanouchi, T. *J. Phys. Chem. Ref. Data* **1977**, *6*, 993.